applied sciences

MDPI

Article

Digital Skin Analysis of Multimodal Skin Rejuvenation with HIFU and Microneedling-Assisted Exosome/PDRN Delivery: A Pilot Comparative Study

Foteini Biskanaki [1,2,*], Athanasia Varvaresou [2], Effie G. Papageorgiou [2], Evaggelia Protopapa [2] and Andreas C. Lazaris [1]

[1] First Department of Pathology, School of Medicine, The National and Kapodistrian University of Athens, 115 27 Athens, Greece; alazaris@med.uoa.gr
[2] Department of Biomedical Sciences, School of Health and Care Sciences, University of West Attica, 28 Ag. Spyridonos Str., Panepistimioupolis Egaleo Park, 122 43 Athens, Greece; avarvares@uniwa.gr (A.V.); efipapag@uniwa.gr (E.G.P.); evi.protopapas@gmail.com (E.P.)
* Correspondence: fbiskanaki@uniwa.gr; Tel.: +30-69-8813-2130

Abstract

Skin aging is associated with collagen degradation, wrinkle formation, enlarged pores, pigmentation changes, and reduced overall skin quality. This pilot comparative clinical study evaluated the short-term effects of HIFU monotherapy, microneedling-assisted EXO-PDRN therapy, and sequential HIFU followed by microneedling-assisted EXO-PDRN using AI-assisted digital skin analysis. Twenty-eight healthy adults aged 45–55 years were allocated into four groups: control, HIFU, MN–EXO-PDRN, and HIFU + MN–EXO-PDRN. Each active monotherapy group received one treatment session, while the combined group received one HIFU session followed seven days later by one microneedling-assisted EXO-PDRN session. Final follow-up assessment was performed at 30–40 days, according to the intervention timeline of each group. The primary descriptive outcome was the median percentage change from baseline. HIFU produced the greatest median reductions in wrinkles (−48.6%) and pores (−49.4%), whereas HIFU + MN–EXO-PDRN demonstrated broader early improvements in sensitivity (−55.9%), wrinkles (−39.3%), pores (−33.3%), UV spots (−19.1%), and global pixel-based skin burden (−29.9%). Control-group increases were interpreted cautiously due to the exploratory design and potential measurement variability. Larger randomized studies with longer follow-up are warranted.

Keywords: high-intensity focused ultrasound (HIFU); microneedling; exosomes; polydeoxyribonucleotide; EXO-PDRN; skin rejuvenation; regenerative aesthetics; digital skin analysis

Academic Editor: Jongsung Lee

Received: 11 June 2026
Revised: 1 July 2026
Accepted: 9 July 2026
Published: 14 July 2026

1. Introduction

Skin aging is a complex biological process characterized by progressive structural and functional alterations of the epidermis and dermis, including collagen degradation, reduced dermal elasticity, dyschromia, enlarged pores, fine lines, wrinkles, and impaired overall skin quality. These changes result from both intrinsic aging mechanisms and extrinsic factors such as ultraviolet (UV) radiation, oxidative stress, chronic inflammation, pollution, and environmental exposure [1,2]. At the molecular level, aged and photoaged skin demonstrates reduced fibroblast activity, extracellular matrix degradation, altered collagen organization, increased matrix metalloproteinase activity, impaired barrier function,

and dysregulated inflammatory signaling pathways [1–3]. Consequently, contemporary aesthetic and regenerative approaches increasingly focus not only on improving visible signs of aging but also on activating biological pathways associated with tissue remodeling, repair, and regeneration.

Non-invasive and minimally invasive aesthetic technologies have gained considerable interest as strategies for facial rejuvenation without the downtime and risks associated with surgical procedures [4]. Among these modalities, High-Intensity Focused Ultrasound (HIFU) is an energy-based technology widely used for skin tightening, lifting, and facial rejuvenation [3–5]. HIFU acts through the conversion of focused acoustic energy into localized thermal coagulation points at selected tissue depths while preserving the epidermal surface. This controlled thermal injury induces immediate collagen contraction and activates wound-healing pathways that may promote neocollagenesis, elastin remodeling, and progressive improvement in skin laxity and firmness [4,5]. Depending on treatment depth, HIFU may target the dermis, subcutaneous tissue, and deeper fibromuscular structures, making it particularly relevant for non-surgical lifting procedures. Recent evidence also suggests that combination protocols integrating HIFU with adjunctive technologies or topical bioactive compounds may further improve skin texture, wrinkles, pores, brightness, hydration, and overall skin quality [4,5]. In addition, increasing evidence suggests that energy-based aesthetic procedures may influence oxidative and inflammatory pathways involved in tissue remodeling and repair, further supporting the biological relevance of regenerative combination protocols [3].

Microneedling is a minimally invasive technique that combines controlled microinjury with enhanced transdermal delivery. By creating multiple temporary microchannels across the stratum corneum and epidermis, microneedling transiently disrupts the skin barrier and facilitates the penetration of topical compounds that would otherwise demonstrate limited diffusion through intact skin [6,7]. Simultaneously, the controlled microinjuries activate physiological wound-healing mechanisms involving inflammatory, proliferative, and remodeling phases, which may stimulate fibroblast activation, growth factor release, collagen and elastin synthesis, and extracellular matrix reorganization [6,7]. For this reason, microneedling has been extensively investigated for skin rejuvenation, enlarged pores, fine wrinkles, dyschromia, acne scars, and as a delivery-enhancement technique for regenerative formulations. In the context of the present study, its importance lies not only in collagen induction but also in its ability to enhance the bioavailability of EXO-PDRN components beyond the stratum corneum barrier.

Exosomes are nanosized extracellular vesicles secreted by cells and recognized as important mediators of intercellular communication. They transport bioactive cargo, including proteins, lipids, metabolites, messenger RNA, and microRNA, capable of influencing the behavior of recipient cells [8]. In skin biology and regenerative aesthetics, exosome-based formulations have attracted increasing interest because they may modulate inflammation, oxidative stress, fibroblast activity, collagen synthesis, angiogenic signaling, extracellular matrix remodeling, wound healing, and tissue repair [9–12]. Emerging clinical evidence suggests potential benefits of exosome-based interventions in photoaging, skin rejuvenation, post-procedure recovery, elasticity, hydration, pigmentation, and acne scar management [9–12]. However, despite their growing popularity, the field remains heterogeneous regarding exosome source, isolation methods, characterization, concentration, dosing, delivery route, and clinical endpoints. Therefore, although exosome-based aesthetics appear promising, current literature highlights the need for standardized protocols and objective outcome evaluation [9,10].

Polydeoxyribonucleotide (PDRN) is a DNA-derived regenerative compound composed of deoxyribonucleotide polymers, commonly purified from fish-derived DNA

sources. Its biological activity has primarily been associated with activation of adenosine A2A receptors, resulting in anti-inflammatory effects, angiogenesis stimulation, fibroblast activation, and tissue repair enhancement [13,14]. In addition, PDRN may support cellular repair through nucleotide salvage pathways involved in DNA synthesis and cellular proliferation. In dermatology and regenerative aesthetics, PDRN has been investigated for wound healing, post-procedure recovery, hydration improvement, fine wrinkles, and overall skin quality enhancement [13,14]. Nevertheless, as with many bioactive macromolecules, topical penetration through intact skin may be limited by the stratum corneum barrier, making penetration-enhancing techniques such as microneedling particularly relevant.

Contemporary regenerative aesthetics increasingly favors multimodal therapeutic approaches that target different anatomical and biological levels of skin aging simultaneously rather than relying on single-modality interventions. Combination protocols may theoretically provide complementary effects by simultaneously promoting collagen remodeling, epidermal renewal, inflammatory modulation, extracellular matrix repair, angiogenic signaling, and enhancement of transdermal bioavailability [4–15]. The rationale for combining HIFU, microneedling, exosome-based formulations, and PDRN is therefore based on their complementary mechanisms of action. HIFU primarily targets deeper dermal and subdermal remodeling through focused thermal stimulation, whereas microneedling induces superficial controlled microinjury and transient microchannels that enhance topical delivery. Exosome-based formulations may support regenerative cell-to-cell signaling, while PDRN may contribute to tissue repair through anti-inflammatory, angiogenic, and fibroblast-supportive mechanisms [8–15]. Consequently, a sequential multimodal protocol combining HIFU with microneedling-assisted EXO-PDRN delivery may theoretically address multiple aspects of skin aging simultaneously, including collagen remodeling, extracellular matrix repair, epidermal renewal, inflammatory modulation, and regenerative signaling.

One of the major challenges in aesthetic medicine is the objective evaluation of treatment outcomes. Although clinical assessment and patient satisfaction remain essential, they are inherently subjective and may be influenced by lighting conditions, photography variability, evaluator bias, and patient expectations. For this reason, digital imaging systems and AI-assisted skin analysis technologies are increasingly incorporated into aesthetic research and clinical practice in order to provide more reproducible and quantifiable assessment of skin quality parameters such as wrinkles, pores, pigmentation, UV-related damage, vascular alterations, and texture irregularities [16–18]. Interestingly, even early biological responses following a single treatment session may produce measurable changes in skin quality parameters during the initial remodeling phase, particularly when objective digital analysis systems are used. Evaluation during the first 3–5 weeks after treatment may therefore capture early collagen remodeling, epidermal turnover, inflammatory modulation, and skin texture changes associated with regenerative signaling pathways.

Despite the increasing clinical use of these technologies in aesthetic practice, direct comparative evidence remains limited. Existing literature generally evaluates HIFU as a monotherapy, microneedling as a remodeling or delivery-enhancement technique, exosome-based formulations as regenerative agents, or HIFU combined with non-exosome topical treatments [4,5,9–12]. Direct comparisons between HIFU monotherapy, microneedling-assisted EXO-PDRN therapy, and their sequential combination using objective AI-supported digital skin analysis remain scarce. Although substantial literature exists regarding HIFU-induced dermal remodeling, microneedling-assisted transdermal delivery, exosome-based regenerative approaches, and PDRN-related skin repair mechanisms individually, comparative evidence regarding sequential multimodal protocols combining these interventions remains limited. In addition, few studies have evaluated such regenerative aesthetic approaches using objective AI-assisted digital skin analysis

systems capable of quantifying multiple skin aging parameters simultaneously. Therefore, the present pilot comparative study aimed to investigate the short-term effects of HIFU, microneedling-assisted EXO-PDRN, and their sequential combination using objective digital skin analysis assessment. Therefore, the aim of this pilot comparative clinical study was to objectively evaluate and compare the early skin remodeling effects of HIFU monotherapy, microneedling-assisted EXO-PDRN therapy, and their sequential combination using AI-assisted digital skin imaging. Specific outcome measures included wrinkles, pores, spots, UV spots, sensitivity, porphyrins, and global pixel-based skin burden as quantitative indicators of skin quality and early treatment response [16–18].

2. Materials and Methods

2.1. Study Design

This pilot comparative clinical study included 28 healthy adult volunteers aged 45–55 years presenting with clinical signs of biological and photoinduced skin aging. Participants were allocated into four equal groups according to the intervention protocol: (i) control group, (ii) HIFU monotherapy group, (iii) microneedling-assisted EXO-PDRN therapy group, and (iv) combined sequential HIFU plus microneedling-assisted EXO-PDRN therapy group. Each group included seven participants.

The study was designed to compare the effects of each active intervention with the control group and to explore whether the sequential combination of HIFU followed by microneedling-assisted EXO-PDRN application could produce greater improvement in objective skin remodeling and rejuvenation parameters. Outcome assessment was performed using AI-assisted digital skin analysis, focusing on wrinkles, pores, spots, UV spots, sensitivity, porphyrins, and global pixel-based skin burden (Figure 1).

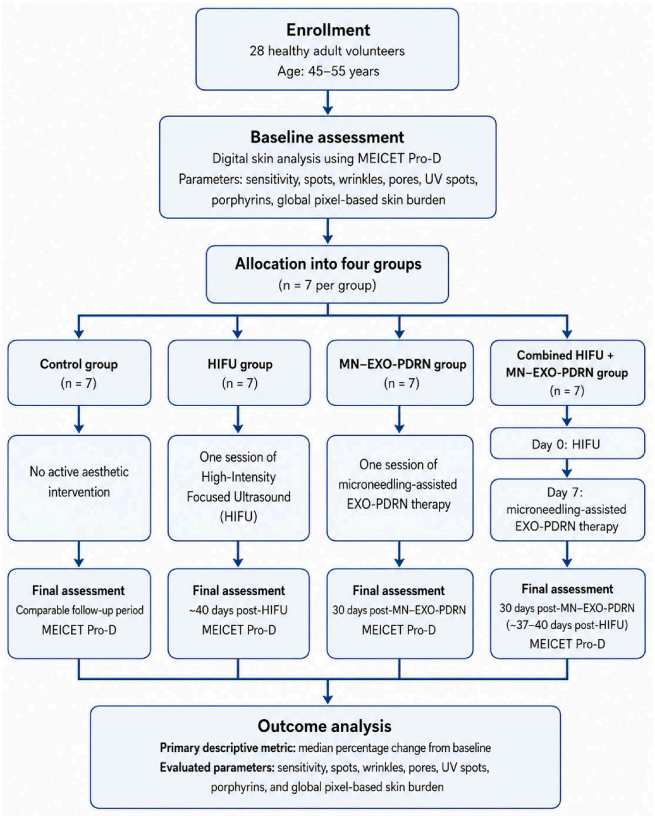

Figure 1. Study design flowchart showing participant allocation, intervention groups, and follow-up assessment in the pilot comparative clinical study.

This pilot study was designed in accordance with methodological principles for pilot and feasibility studies, emphasizing preliminary effect estimation, feasibility assessment, and generation of data for future larger-scale controlled trials [19,20].

2.2. Participants

A total of 28 healthy adult volunteers aged 45–55 years were enrolled in the study, including 24 women and 4 men. All participants presented visible signs of biological and photoinduced skin aging, including fine lines, wrinkles, enlarged pores, uneven skin texture, pigmentation-related changes, and reduced overall skin quality.

Participants were allocated into four equal groups of seven individuals according to the intervention protocol: (i) control group, receiving no active aesthetic intervention; (ii) HIFU group, receiving one session of High-Intensity Focused Ultrasound; (iii) MN–EXO-PDRN group, receiving one session of microneedling-assisted EXO-PDRN therapy; and (iv) HIFU + MN–EXO-PDRN group, receiving one session of HIFU followed seven days later by microneedling-assisted EXO-PDRN therapy.

The demographic distribution was considered appropriate for a pilot comparative study aiming to generate preliminary clinical and quantitative data on skin rejuvenation outcomes in middle-aged adults with visible signs of skin aging.

2.3. Inclusion and Exclusion Criteria

Eligible participants were healthy adults aged 45–55 years with visible signs of biological and/or photo-induced skin aging who were willing to undergo digital skin analysis before and after the intervention. Participants were also required to avoid additional aesthetic procedures or topical/interventional anti-aging treatments during the study period. Participants were instructed not to initiate any new topical skincare products, sunscreens, or cosmetic treatments during the study period and to maintain their usual skincare routine throughout follow-up. No standardized topical cream or sunscreen was provided by the study team.

Exclusion criteria included active skin infection, inflammatory dermatoses in the treatment area, recent facial aesthetic procedures, pregnancy or breastfeeding, history of keloid or hypertrophic scarring, uncontrolled systemic disease, use of photosensitizing medication, recent isotretinoin use, implanted electronic devices, metal implants in the treatment area, previous HIFU or microneedling treatment within the last 6 months, and any contraindication to HIFU or microneedling.

2.4. Ethical Considerations and Informed Consent

The study was conducted in accordance with the Declaration of Helsinki and approved by the Bioethics and Ethics Committee of the Medical School of the National and Kapodistrian University of Athens, Greece (Approval No. 1249/29.06.2026). A subsequent amendment to the research protocol, including the additional microneedling-assisted EXO-PDRN intervention arms, was submitted to the same Committee and received protocol registration No. 1249/26.05.2026. The amendment was approved by the Committee prior to implementation. Written informed consent was obtained from all participants prior to inclusion in the study. Written informed consent was also obtained for the publication of anonymized clinical photographs and digital skin analysis images.

2.5. HIFU Protocol

Participants received treatment using a CE-marked HIFU device equipped with 1.5 mm, 3.0 mm, and 4.5 mm transducers. Treatment was performed on the facial and neck regions according to standard aesthetic safety procedures and individualized skin assessment. Focused ultrasound energy was delivered at selected tissue depths to induce

controlled thermal stimulation, collagen contraction, and subsequent dermal remodeling [5–7]. The epidermal surface was preserved, and no ablative injury was performed.

All HIFU procedures were performed by the first author, an experienced practitioner with more than eight years of daily clinical practice and academic training in aesthetic and biomedical applications. Each participant underwent a single treatment session lasting approximately 40–60 min, with short breaks provided as needed according to the treatment area and participant comfort.

No topical anesthetic cream or injectable anesthesia was used. Participant comfort was supported through a non-pharmacological comfort protocol, including continuous verbal communication, reassurance, relaxing background music, and the use of a handheld anti-stress ball during the procedure.

HIFU transducers operating at 2–3 MHz were selected according to the target anatomical depth. Depths of 3.0–4.5 mm were used for the neck and cheeks, whereas depths of 1.5–3.0 mm were used for the periorbital region and forehead. Treatment settings were selected according to anatomical area, skin thickness, degree of laxity, and participant tolerance. The commercial brand name of the HIFU device was not reported in order to avoid promotional or commercial bias. All procedures followed standard safety guidelines for aesthetic HIFU application.

Treatment parameters included an energy range of 0.6–1.2 J per shot, where measurable. The treatment sequence was neck, cheeks, periorbital region, and forehead. The total number of shots per participant ranged from 390 to 480 for the face and neck.

2.6. Microneedling-Assisted EXO-PDRN Protocol

Participants allocated to the microneedling-assisted EXO-PDRN group received a single treatment session using the Micropen EVO® device (Revance, Dallas, TX, USA). Prior to treatment, medical history was obtained to identify contraindications and document baseline skin characteristics.

The treatment area was cleansed using a non-irritating cleanser to prepare the skin while minimizing unnecessary irritation. A commercially available exosome–PDRN formulation was used as the professional topical regenerative formulation. Product composition and application procedures followed the manufacturer's professional protocol, while the biological rationale for exosome- and PDRN-based skin regeneration was supported by published literature [8–14].

A sterile, water-soluble professional hydrogel (Skinfuse® Lift HG, Crown Aesthetics, Dallas, TX, USA) was used as a glide medium during the procedure. The hydrogel was applied to facilitate smooth device movement, maintain skin hydration, prevent cartridge obstruction, and improve procedural comfort.

Microneedling was performed according to the manufacturer's protocol for the management of wrinkles and fine lines. A standardized needle depth of 0.5 mm was selected for all participants. This depth was chosen because superficial-to-medium microneedling depths (approximately 0.25–0.5 mm) may enhance the penetration and bioavailability of exosome-based and PDRN-containing formulations while avoiding excessive tissue trauma, significant bleeding, or intense inflammatory response [10,11]. The objective was to create controlled superficial microchannels rather than deep tissue injury.

The treatment technique was standardized for all participants. Two passes were performed over the treated areas, although the manufacturer's protocol allows up to three passes. The optional third pass was intentionally omitted because all volunteers were undergoing their first microneedling session, and uniform treatment parameters were considered essential for study consistency. Treatment was performed using controlled

linear and overlapping passes across the facial treatment areas, with attention to consistent pressure, speed, and coverage.

Approximately 3 mL of the exosome–PDRN formulation was used during the in-clinic procedure. Approximately 2 mL was applied progressively during microneedling to facilitate contact of the formulation with the transient microchannels. Following completion of the procedure, an additional 1 mL was applied topically to support post-procedure absorption and regenerative activity. Participants were also provided with approximately 2 mL of the formulation for home use during the subsequent 2–3 days, applied twice daily (morning and evening) according to standardized post-treatment instructions.

No topical anesthetic cream or injectable anesthesia was used. Participant comfort was supported through a non-pharmacological comfort protocol consisting of continuous verbal communication, reassurance, relaxing background music, and the use of a handheld anti-stress ball during the procedure. Pain and discomfort were assessed using a 0–10 numerical rating scale, with a mean reported discomfort score of approximately 6.

Immediately after treatment, a sterile biocellulose mask was applied for approximately 20 min to all participants to support skin soothing, hydration, barrier recovery, and post-procedure comfort. Following mask removal, the exosome–PDRN formulation and hydrogel were reapplied topically to support hydration, skin comfort, and barrier recovery.

2.7. Combined Sequential HIFU + MN–EXO-PDRN Protocol

Participants in the combined treatment group first received one session of HIFU according to the standardized HIFU protocol described above. Seven days later, repeat digital skin assessment was performed using the MEICET Pro-D system, followed by microneedling-assisted EXO-PDRN therapy using the same protocol described for the MN-EXO-PDRN group. Final post-treatment assessment was performed 30 days after EXO-PDRN application, corresponding to approximately 37–40 days after HIFU treatment.

This sequential multimodal approach was designed to combine deeper energy-based dermal remodeling induced by HIFU with superficial controlled microinjury and enhanced regenerative topical delivery induced by microneedling [6,10,11]. The protocol was based on the hypothesis that sequential treatment may target multiple anatomical and biological levels of skin aging simultaneously, including collagen remodeling, epidermal renewal, inflammatory modulation, and regenerative signaling pathways.

The seven-day interval between HIFU and microneedling-assisted EXO-PDRN application was selected to allow an initial post-HIFU tissue response and early remodeling activity before the subsequent regenerative topical delivery procedure.

2.8. Digital Skin Analysis

Digital skin analysis was performed at baseline and at final follow-up using the MEICET Pro-D skin analyzer (MEICET, Guangzhou, China). Digital skin imaging systems have been used in aesthetic and dermatological research to provide objective and reproducible assessment of facial skin parameters, including spots, wrinkles, texture, pores, UV spots, pigmentation-related features, red areas, and porphyrins [16–18]. Fitzpatrick skin phototype was recorded as part of each participant's baseline history and digital skin analysis profile in the MEICET Pro-D system.

In the HIFU group, the final assessment was performed approximately 40 days after HIFU treatment. In the MN–EXO-PDRN group, the final assessment was performed 30 days after microneedling-assisted EXO-PDRN application. In the combined HIFU + MN–EXO-PDRN group, HIFU was performed first, followed seven days later by microneedling-assisted EXO-PDRN therapy; final assessment was performed 30 days after EXO-PDRN

application, corresponding to approximately 37–40 days after HIFU. The control group was reassessed after a comparable follow-up period.

The evaluated skin parameters included sensitivity, spots, wrinkles, pores, UV spots, porphyrins, and global pixel-based skin burden. All measurements were obtained using the same device and under comparable environmental and imaging conditions, including standardized facial positioning, lighting, camera distance, and participant positioning. The same assessment protocol was followed for all participants to reduce measurement variability and improve reproducibility.

2.9. Outcome Measures

The primary descriptive outcome was the median percentage change from baseline to final follow-up in AI-assisted digital skin analysis parameters. Percentage change was calculated individually for each participant as follows: [(follow-up value − baseline value)/baseline value] × 100. The evaluated parameters included sensitivity, spots, wrinkles, pores, UV spots, porphyrins, and global pixel-based skin burden.

Secondary descriptive outcomes included baseline and follow-up values for each parameter, which were presented as complementary descriptive data. The main analysis compared each active treatment group with the control group, while additional exploratory comparisons were performed among HIFU monotherapy, microneedling-assisted EXO-PDRN therapy, and the combined sequential HIFU + MN–EXO-PDRN protocol.

2.10. Statistical Analysis

Data were analyzed using descriptive and comparative statistics. Continuous variables were expressed as mean ± standard deviation (SD) and median with interquartile range (IQR), where appropriate. Given the exploratory pilot design and the small sample size in each group, median percentage change from baseline was defined as the primary descriptive metric for interpreting treatment-related effects. Mean-based baseline and follow-up values were retained as complementary descriptive data and were not used as the primary basis for efficacy interpretation.

Given the pilot design and the small sample size per group, non-parametric statistical methods were used. Within-group differences between baseline and post-treatment values were assessed using the Wilcoxon signed-rank test. Between-group comparisons of percentage changes among the four groups were performed using the Kruskal–Wallis test. When appropriate, exploratory pairwise comparisons were conducted between each active treatment group and the control group, as well as between the combined sequential protocol and the two monotherapy groups.

A two-sided p-value < 0.05 was considered statistically significant. Due to the exploratory nature of this pilot study, no a priori sample size calculation was performed, and findings were interpreted as preliminary in accordance with recommendations for pilot and feasibility studies [19,20]. All statistical analyses were performed using IBM SPSS Statistics for Windows, version 26.0 (IBM Corp., Armonk, NY, USA).

3. Results

3.1. Participant Characteristics

A total of twenty-eight healthy adult volunteers completed the study. The study population consisted of twenty-four women and four men, allocated into four equal groups of seven participants: control, HIFU monotherapy, microneedling-assisted EXO-PDRN therapy, and combined sequential HIFU plus microneedling-assisted EXO-PDRN therapy. The control group included six women and one man and did not receive any active aesthetic intervention.

Baseline demographic and lifestyle characteristics of participants aged 45–55 years are presented in Table 1. These included age, sex, smoking status, sunscreen use, sun exposure habits, alcohol consumption, physical activity, water intake, self-reported stress levels, medication use, and previous exposure to HIFU treatment. Overall, the cohort represented a clinically stable middle-aged population with visible signs of biological and photoinduced skin aging and without uncontrolled systemic or active dermatologic disease. Regarding Fitzpatrick skin phototype, 27 participants were recorded as phototype III, while one male participant in the MN–EXO-PDRN group was recorded as phototype VI. Fitzpatrick phototype was documented as part of each participant's baseline history and digital skin analysis profile.

Table 1. Baseline demographic and lifestyle characteristics of study participants aged 45–55 years.

Characteristic	Control (n = 7)	HIFU (n = 7)	MN–EXO-PDRN (n = 7)	HIFU & MN–EXO-PDRN (n = 7)	Total (n = 28)
Female	6	6	6	6	24
Male	1	1	1	1	4
Fitzpatrick phototype III	7	7	6	7	27
Fitzpatrick phototype VI	0	0	1	0	1
Smokers	2	2	1	2	7
Regular sunscreen use	4	5	5	4	18
High sun exposure	3	2	3	3	11
Alcohol consumption	2	3	2	2	9
Physical activity	3	3	4	3	13
Adequate water intake	4	4	5	4	17
Moderate/high stress	5	4	5	4	18
Medication use	1	1	0	1	3
Previous HIFU	0	0	0	0	0
Previous MN–EXO-PDRN	0	0	0	0	0

Note: Values are presented as number of participants unless otherwise indicated. Fitzpatrick skin phototype was recorded as part of each participant's baseline history and MEICET Pro-D digital skin analysis profile.

3.2. Baseline and Follow-Up Digital Skin Analysis

Baseline and final follow-up digital skin analysis parameters for all study groups are presented in Table 2. The evaluated parameters included sensitivity, spots, wrinkles, pores, UV spots, porphyrins, and global pixel-based skin burden. Baseline values varied among participants, reflecting the heterogeneous clinical presentation of biological and photoinduced skin aging in the study population.

Table 2. Baseline and final follow-up descriptive values of AI-assisted digital skin analysis parameters.

Parameter	Group	Baseline Mean ± SD	Final Mean ± SD	p-Value
Sensitivity	HIFU + MN–EXO-PDRN	29.55 ± 16.65	16.09 ± 14.49	0.0156
	HIFU	21.58 ± 16.00	16.92 ± 11.99	0.0781
	MN–EXO-PDRN	32.08 ± 22.25	23.02 ± 17.15	0.0156
	Control	17.60 ± 16.32	22.31 ± 18.72	0.0156
Spots	HIFU + MN–EXO-PDRN	11.79 ± 1.96	9.42 ± 2.27	0.0156
	HIFU	12.71 ± 2.33	10.52 ± 2.55	0.1094
	MN–EXO-PDRN	12.39 ± 3.90	10.62 ± 3.61	0.0156
	Control	10.79 ± 2.83	12.27 ± 3.00	0.0156
Wrinkles	HIFU + MN–EXO-PDRN	752.00 ± 207.66	470.57 ± 148.93	0.0156
	HIFU	1687.43 ± 369.97	1027.29 ± 536.78	0.0312
	MN–EXO-PDRN	679.14 ± 305.19	490.14 ± 172.35	0.1094
	Control	599.00 ± 139.25	721.57 ± 125.68	0.0156

Table 2. *Cont.*

Parameter	Group	Baseline Mean ± SD	Final Mean ± SD	*p*-Value
Pores	HIFU + MN–EXO-PDRN	2235.71 ± 692.73	1639.14 ± 839.78	0.0156
	HIFU	3195.71 ± 678.56	1767.86 ± 702.11	0.0156
	MN–EXO-PDRN	2549.29 ± 1151.77	1965.86 ± 797.78	0.2188
	Control	2139.43 ± 994.92	2250.71 ± 969.64	0.0156
UV Spots	HIFU + MN–EXO-PDRN	13.52 ± 2.82	12.08 ± 3.66	0.1094
	HIFU	18.63 ± 4.66	13.39 ± 3.41	0.0156
	MN–EXO-PDRN	14.61 ± 2.95	14.37 ± 2.11	0.9375
	Control	12.98 ± 3.28	14.09 ± 2.97	0.4688
Porphyrins	HIFU + MN–EXO-PDRN	71.29 ± 53.58	47.86 ± 50.81	0.3750
	HIFU	252.57 ± 205.28	162.00 ± 131.86	0.1562
	MN–EXO-PDRN	49.43 ± 52.26	37.43 ± 49.81	0.2656
	Control	87.00 ± 69.04	67.14 ± 39.75	1.0000
Global Pixel-Based Skin Burden	HIFU + MN–EXO-PDRN	43,544.86 ± 13,695.79	27,669.71 ± 9543.91	0.0156
	HIFU	58,920.00 ± 10,892.51	46,328.00 ± 16,285.25	0.1094
	MN–EXO-PDRN	33,417.71 ± 13,046.64	26,055.43 ± 8299.87	0.1562
	Control	33,521.86 ± 9813.50	37,565.14 ± 11,863.00	0.0156

Note: Values are presented as mean ± standard deviation (SD). Baseline and follow-up values are provided as complementary descriptive data and were not used as the primary basis for efficacy interpretation. *p*-values refer to within-group baseline versus final follow-up comparisons using the Wilcoxon signed-rank test. *p*-values refer to within-group baseline versus final follow-up comparisons using the Wilcoxon signed-rank test.

Baseline and follow-up values are presented as complementary descriptive data, whereas the main interpretation of treatment-related effects is based on median percentage changes from baseline, as presented in Table 3. This approach was selected because of the exploratory pilot design and the small sample size in each group.

Table 3. Median percentage change in digital skin analysis parameters across study groups from baseline to final follow-up.

Parameter	Control	HIFU	MN–EXO-PDRN	HIFU + MN–EXO-PDRN	*p*-Value
Sensitivity	+22.3%	−5.2%	−28.7%	−55.9%	0.0003
Spots	+15.8%	−25.4%	−12.6%	−13.9%	0.0079
Wrinkles	+24.0%	−48.6%	−23.0%	−39.3%	0.0037
Pores	+2.7%	−49.4%	−18.7%	−33.3%	0.0010
UV Spots	+0.1%	−26.0%	−2.2%	−19.1%	0.0057
Porphyrins	+1.6%	−46.0%	−40.9%	−25.0%	0.514
Global pixel-based skin burden	+6.3%	−25.9%	−18.4%	−29.9%	0.0159

Note: Values represent median percentage change from baseline. Percentage change was calculated individually for each participant as [(follow-up value − baseline value)/baseline value] × 100. Negative values indicate a reduction in the measured parameter, whereas positive values indicate an increase. Between-group comparisons were performed using the Kruskal–Wallis test. Median percentage change was used as the primary descriptive metric for interpreting treatment-related effects. Porphyrin-related changes in the HIFU group should be interpreted cautiously due to a baseline value of zero in one participant.

Across the active intervention groups, follow-up values generally showed favorable changes in several AI-assisted digital skin analysis parameters compared with the control group. However, mean-based baseline and follow-up values were not used as the primary basis for efficacy interpretation. Treatment-related effects are therefore described primarily in Section 3.4 using median percentage changes from baseline.

3.3. Correlation Analysis of Digital Skin Parameters

Correlation analysis was performed to explore associations among individual percentage changes in AI-assisted digital skin analysis parameters (Figure 2). The strongest correlation was observed between wrinkle-related changes and changes in global pixel-based skin burden (Spearman rho = 0.903, $p < 0.001$), suggesting that changes in wrinkle-related

parameters were closely associated with broader changes in overall digital skin burden. Significant positive correlations were also observed between pore-related changes and global pixel-based skin burden changes (rho = 0.635, p = 0.0003), as well as between sensitivity-related changes and global pixel-based skin burden changes (rho = 0.579, p = 0.0012).

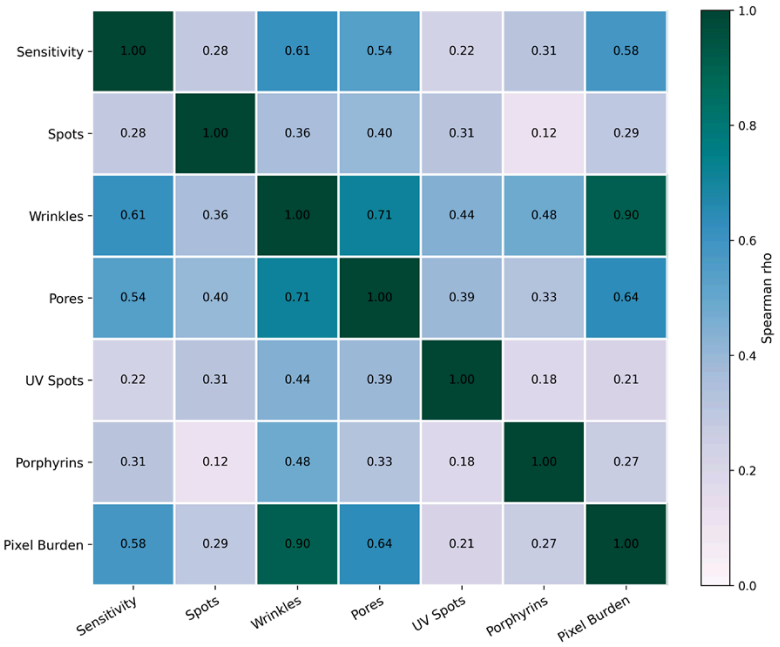

Figure 2. Spearman correlation heatmap of individual percentage changes in digital skin analysis parameters following treatment interventions. Rows and columns represent the evaluated skin parameters, and each cell shows the Spearman correlation coefficient between individual percentage changes in two parameters. Higher positive values indicate stronger parallel changes between parameters. Rows and columns represent individual percentage changes in digital skin analysis parameters. Higher positive values indicate stronger parallel changes between parameters.

The correlation between spot-related changes and UV spot-related changes was weaker and did not reach statistical significance (rho = 0.314, p = 0.1035). Overall, these findings suggest that changes in wrinkles, pores, and sensitivity tended to occur in parallel with broader changes in objective digital skin aging indices, particularly global pixel-based skin burden (Figure 3).

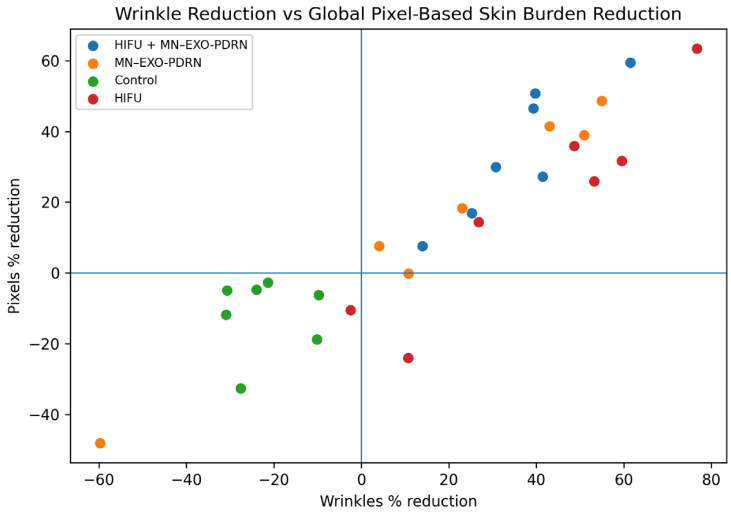

Figure 3. Scatter plot illustrating the correlation between individual percentage changes in wrinkle-related parameters and global pixel-based skin burden across all groups.

3.4. Between-Group Comparison of Median Percentage Changes

Between-group comparisons of median percentage changes from baseline demonstrated statistically significant differences across multiple AI-assisted digital skin analysis parameters (Table 3; Figure 4). Median percentage change from baseline was used as the primary descriptive metric for interpreting treatment-related effects.

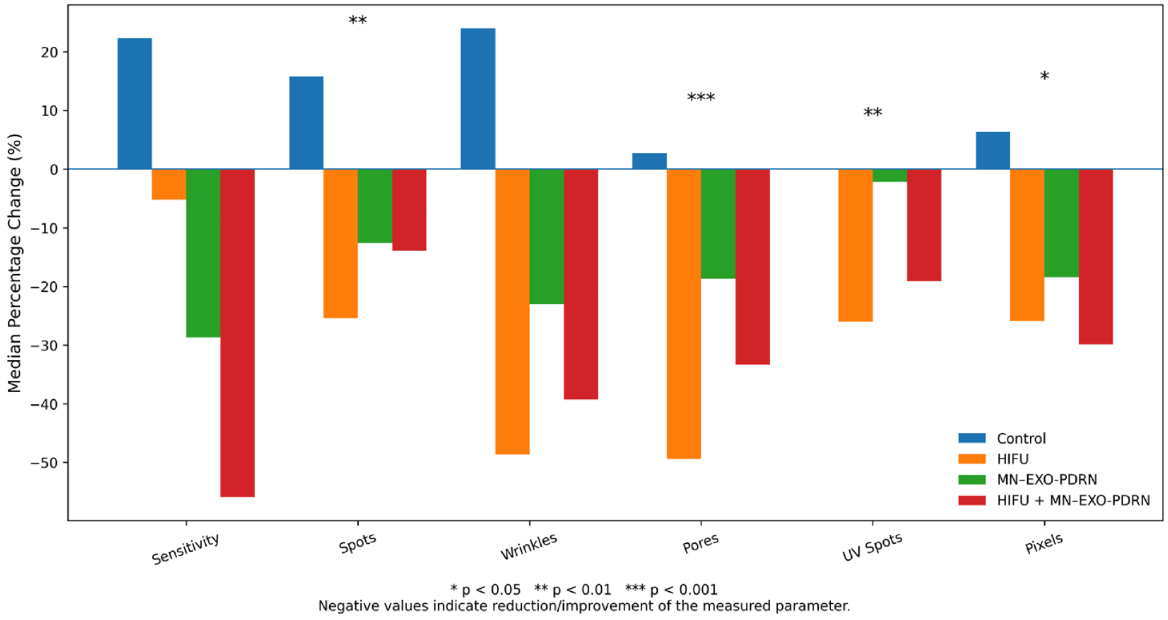

Figure 4. Median percentage changes in digital skin analysis parameters across study groups. Negative values indicate reduction in the measured parameter, whereas positive values indicate an increase. Statistically significant between-group differences were observed for sensitivity, wrinkles, pores, spots, UV spots, and global pixel-based skin burden.

The control group generally demonstrated increasing trends or minimal change during the follow-up period, whereas all active intervention groups showed reductions in several skin aging indices. These control-group changes should be interpreted cautiously, as they may reflect measurement variability, short-term intra-individual skin fluctuations, environmental exposure, hydration status, and the exploratory nature of image-based skin analysis in a small pilot sample.

The HIFU group demonstrated the greatest median reductions in wrinkles (−48.6%), pores (−49.4%), UV spots (−26.0%), and porphyrins (−46.0%), suggesting a pronounced effect on structural and remodeling-related parameters. The MN–EXO-PDRN group demonstrated moderate median reductions mainly in sensitivity (−28.7%), wrinkles (−23.0%), pores (−18.7%), spots (−12.6%), and global pixel-based skin burden (−18.4%).

The combined sequential HIFU + MN–EXO-PDRN group demonstrated a broader early improvement profile across multiple evaluated parameters, particularly sensitivity (−55.9%), wrinkles (−39.3%), pores (−33.3%), UV spots (−19.1%), and global pixel-based skin burden (−29.9%). These findings suggest that the sequential protocol may provide complementary effects across both structural and global skin-quality parameters (Figure 5).

Statistically significant between-group differences were identified for sensitivity ($p = 0.0003$), spots ($p = 0.0079$), wrinkles ($p = 0.0037$), pores ($p = 0.0010$), UV spots ($p = 0.0057$), and global pixel-based skin burden ($p = 0.0159$). Differences in porphyrin-related parameters did not reach statistical significance ($p = 0.514$).

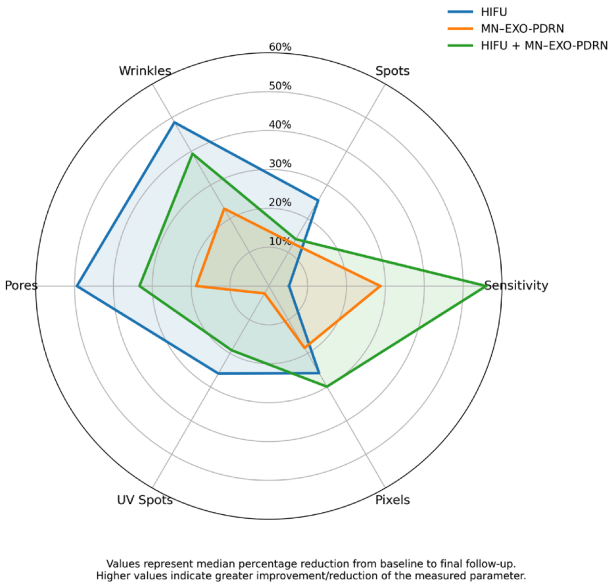

Figure 5. Radar chart illustrating the comparative improvement profile across major digital skin parameters for HIFU, MN–EXO-PDRN, and sequential HIFU + MN–EXO-PDRN interventions. Values represent the magnitude of median percentage reduction for each evaluated parameter. The combined protocol demonstrated a broader overall improvement profile across multiple digital skin aging indices.

3.5. Wrinkle-Related Parameter Changes

Wrinkle-related parameters demonstrated statistically significant between-group differences among the four study groups. The control group showed a median increase in wrinkle-related values (+24.0%) during the observation period. In contrast, all active intervention groups demonstrated reductions in wrinkle-related digital skin burden.

The HIFU monotherapy group demonstrated the greatest median reduction in wrinkles (−48.6%), followed by the combined sequential HIFU + MN–EXO-PDRN group (−39.3%) and the MN–EXO-PDRN group (−23.0%). Between-group comparison was statistically significant ($p = 0.0037$).

These findings suggest that HIFU monotherapy and the combined sequential protocol were associated with marked reductions in wrinkle-related digital skin parameters, while the combined protocol additionally demonstrated broader early improvement across other evaluated skin aging indices.

3.6. Additional AI-Assisted Digital Skin Analysis Parameters

Additional AI-assisted digital skin analysis parameters demonstrated statistically significant between-group differences for pores, spots, UV spots, sensitivity, and global pixel-based skin burden. The HIFU group demonstrated the greatest median reductions in pores (−49.4%) and UV spots (−26.0%), whereas the combined sequential HIFU + MN–EXO-PDRN group demonstrated broader overall improvement across multiple parameters, particularly sensitivity (−55.9%), pores (−33.3%), and global pixel-based skin burden (−29.9%). The MN–EXO-PDRN group demonstrated moderate reductions mainly in sensitivity, spots, pores, and global pixel-based skin burden.

In contrast, the control group generally demonstrated increasing trends or minimal change across most parameters during follow-up. Significant between-group differences were observed for sensitivity ($p = 0.0003$), pores ($p = 0.0010$), spots ($p = 0.0079$), UV spots ($p = 0.0057$), and global pixel-based skin burden ($p = 0.0159$). Porphyrin-related parameters showed variable responses among groups and did not reach statistical significance ($p = 0.514$).

These findings suggest that the active intervention protocols, particularly the sequential multimodal protocol, were associated with broader objective improvement in multiple digital skin aging indices. However, changes in pigmentary indices, including spots and UV spots, should be interpreted as exploratory secondary findings rather than as primary pigment-targeting outcomes. Representative clinical and digital skin analysis images are presented in Figures 6–10.

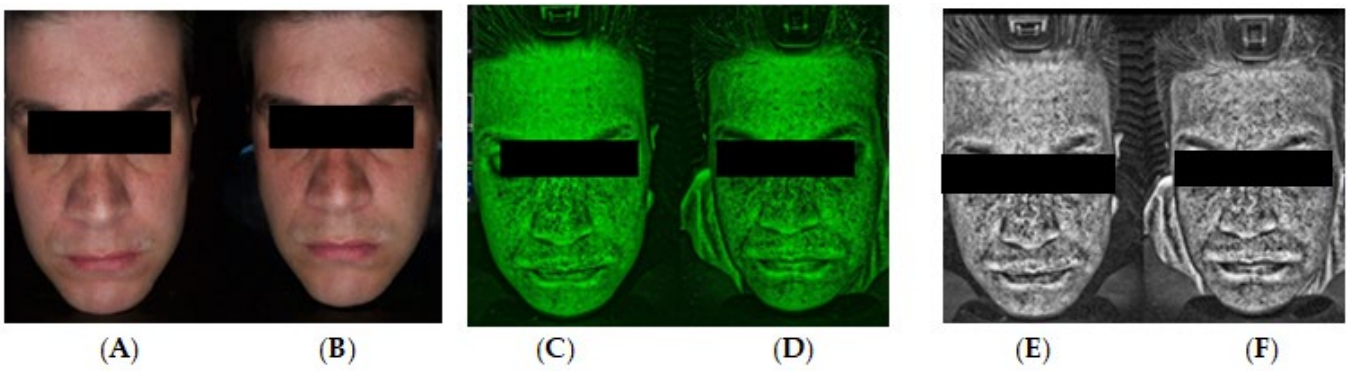

Figure 6. Representative control participant (45-year-old male) who did not receive HIFU, microneedling, or any other aesthetic intervention during the study period. (**A**) Clinical photograph at baseline (timepoint 0). (**B**) Clinical photograph at 40-day follow-up. (**C**) MEICET Pro-D Green Light analysis at baseline (**D**) MEICET Pro-D Green Light Analysis images at 40-day follow-up. (**E**) MEICET Pro-D monochrome/grayscale analysis at baseline. (**F**) MEICET Pro-D monochrome/grayscale analysis at 40-day follow-up. Green light analysis enhances visualization of vascular-related features, erythema distribution, skin tone irregularities, and superficial skin changes that may not be readily visible under standard illumination. Monochrome/grayscale analysis enhances visualization of skin texture, wrinkles, pores, and surface irregularities, while the green marker overlay indicates digitally mapped facial analysis points used for objective skin parameter assessment. An apparent increase in selected digital skin aging parameters was observed after 40 days, which should be interpreted cautiously in the context of short-term measurement variability.

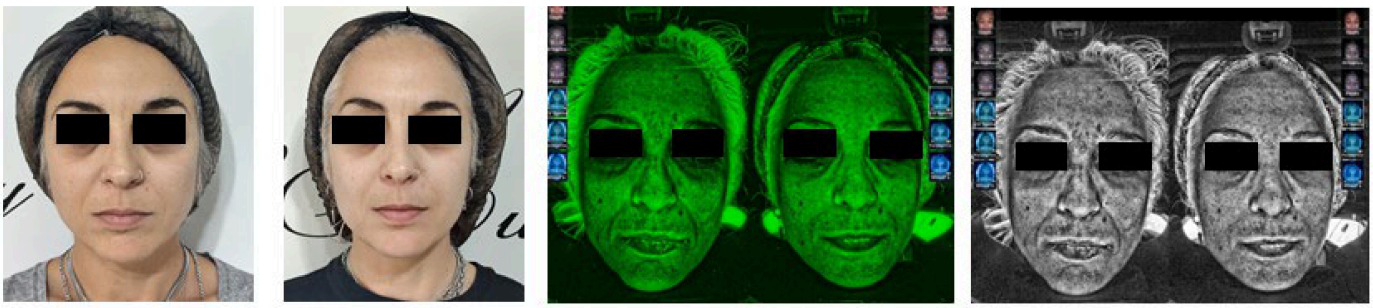

Figure 7. Representative participant (45-year-old female) who received only one treatment with microneedling-assisted EXO-PDRN. (**A**) Clinical photograph at baseline (timepoint 0). (**B**) Clinical photograph at 40-day follow-up. (**C**) MEICET Pro-D Green Light analysis images at baseline (**D**) MEICET Pro-D Green Light Analysis images at 40-day follow-up. (**E**) MEICET Pro-D monochrome/grayscale analysis at baseline. (**F**) MEICET Pro-D monochrome/grayscale analysis at 40-day follow-up. Improvement in skin texture, skin uniformity, and overall skin quality can be observed at follow-up.

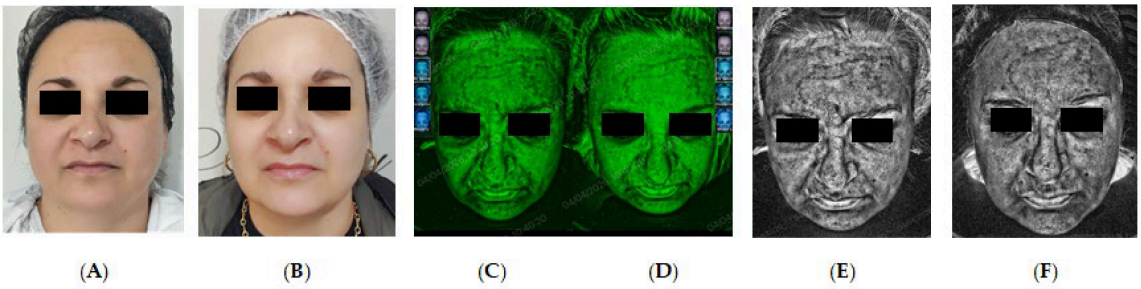

Figure 8. Representative participant (45-year-old female) who received a single HIFU treatment session. (**A**) Clinical photograph at baseline (timepoint 0). (**B**) Clinical photograph at 40-day follow-up. (**C**) MEICET Pro-D Green Light Analysis image at baseline. (**D**) MEICET Pro-D Green Light Analysis image at 40-day follow-up. (**E**) MEICET Pro-D monochrome/grayscale analysis at baseline. (**F**) MEICET Pro-D monochrome/grayscale analysis at 40-day follow-up. Visible improvement in skin texture, wrinkle-related parameters, and overall skin quality can be observed at follow-up.

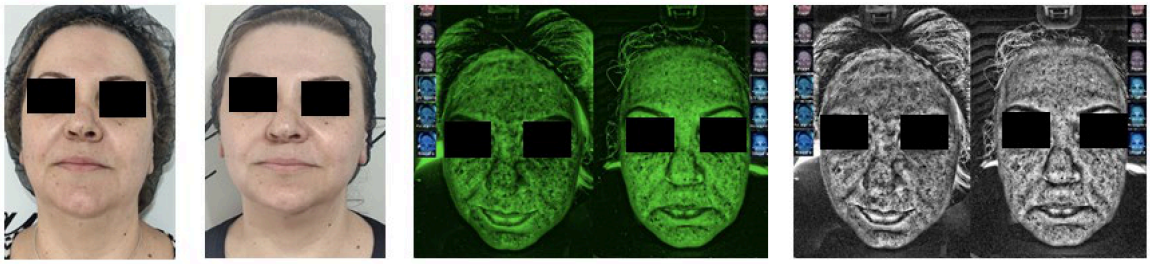

Figure 9. Representative participant (45-year-old female) who received sequential HIFU + microneedling-assisted EXO-PDRN treatment. Microneedling-assisted EXO-PDRN was performed 7 days after HIFU. (**A**) Clinical photograph at baseline (timepoint 0). (**B**) Clinical photograph at 40-day follow-up. (**C**) MEICET Pro-D Green Light Analysis image at baseline. (**D**) MEICET Pro-D Green Light Analysis image at 40-day follow-up. (**E**) MEICET Pro-D monochrome/grayscale analysis at baseline. (**F**) MEICET Pro-D monochrome/grayscale analysis at 40-day follow-up. Representative images demonstrate visible improvement in skin texture, skin uniformity, pore appearance, wrinkle-related parameters, and overall skin quality following the sequential multimodal treatment protocol.

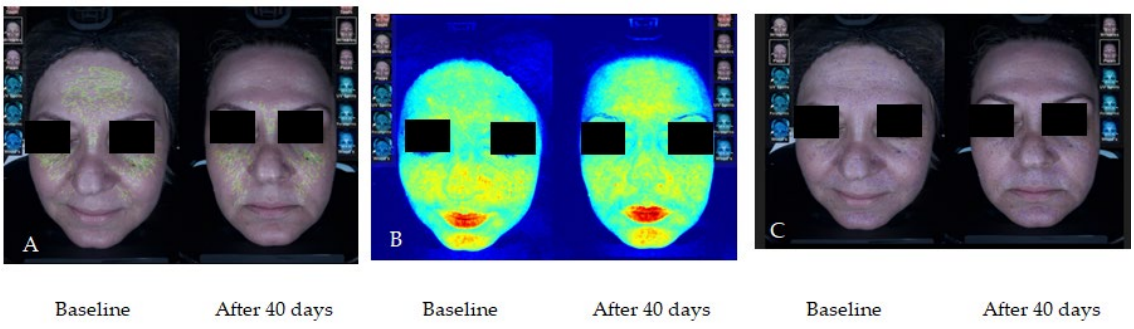

Figure 10. Representative participant (45-year-old female) who received sequential HIFU + microneedling-assisted EXO-PDRN treatment. Microneedling-assisted EXO-PDRN was performed 7 days after HIFU. (**A**) MEICET Pro-D aging analysis at baseline and 40-day follow-up. (**B**) MEICET Pro-D color-mapping analysis at baseline and 40-day follow-up. Color-mapping analysis highlights regional variations in skin tone and digital skin burden, with warmer colors indicating greater intensity of the analyzed parameter and cooler colors indicating lower intensity. (**C**) MEICET Pro-D pore analysis at baseline and 40-day follow-up. Representative images demonstrate improvement in facial oval appearance, skin texture uniformity, pore-related features, and overall digital skin quality at follow-up.

Representative MEICET Pro-D images demonstrated visible changes across multiple imaging modes and digital skin analysis parameters following the active intervention protocols. Although improvements were observed after both HIFU monotherapy and microneedling-assisted EXO-PDRN therapy, the sequential HIFU + MN–EXO-PDRN protocol appeared to provide a broader improvement profile, with visible changes in aging-related features, skin tone distribution, pore-related parameters, texture uniformity, and overall facial oval appearance (Figure 10). These representative findings visually support the quantitative results, suggesting that the combined protocol may provide multiple complementary benefits across different levels of skin assessment.

3.7. Safety

All procedures were completed without serious adverse events or treatment discontinuation. No topical anesthetic cream or injectable anesthesia was used during either HIFU or microneedling procedures.

Participant discomfort during microneedling-assisted EXO-PDRN application was generally mild to moderate, with a mean reported discomfort score of approximately 6 on a 0–10 numerical rating scale. Discomfort during HIFU treatment was transient and well tolerated.

Expected transient erythema, mild edema, and temporary skin sensitivity were observed immediately after treatment in some participants and resolved spontaneously within a short period without complications or medical intervention. No infections, scarring, pigmentary complications, burns, or persistent adverse effects were observed during the follow-up period.

Overall, the treatment protocols demonstrated a favorable short-term safety and tolerability profile within the limitations of this pilot study. Immediately post-treatment clinical appearance differed between HIFU and microneedling-assisted EXO-PDRN interventions. Immediately after HIFU treatment, minimal visible erythema or epidermal irritation was observed despite deep thermal tissue stimulation. In contrast, microneedling-assisted EXO-PDRN produced transient diffuse erythema immediately after treatment, consistent with controlled superficial microinjury and early wound-healing activation (Figure 11).

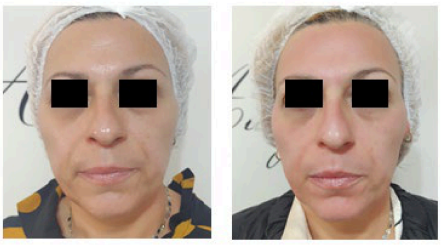

Figure 11. (**A**) Representative immediate post-treatment images following HIFU and (**B**) microneedling-assisted EXO-PDRN, demonstrating transient erythema and expected treatment-related skin responses without serious adverse events.

4. Discussion

The present pilot comparative clinical study evaluated the short-term effects of HIFU monotherapy, microneedling-assisted EXO-PDRN therapy, and sequential HIFU followed by microneedling-assisted EXO-PDRN treatment on objective AI-assisted digital skin aging parameters. The main finding was that all active interventions demonstrated measurable changes compared with the control group, while the combined sequential HIFU + MN–EXO-PDRN protocol showed a broader early improvement profile across

multiple digital skin parameters. Given the pilot design and small sample size, these findings should be interpreted as preliminary and hypothesis-generating.

A key strength of this pilot study is its comparative four-arm design, which allowed the evaluation of HIFU alone, microneedling-assisted EXO-PDRN therapy alone, their sequential combination, and a control group under the same digital skin analysis framework. This design addresses an important gap in the current literature, as most available studies focus on single-modality interventions rather than direct comparisons of sequential multimodal protocols. Therefore, the present study provides preliminary comparative evidence on how deeper energy-based remodeling, superficial controlled microinjury, and regenerative topical delivery may contribute differently to measurable skin rejuvenation outcomes.

The combined HIFU + MN–EXO-PDRN group demonstrated favorable early changes in sensitivity, wrinkles, pores, UV spots, and global pixel-based skin burden. However, the pattern of response differed among treatment arms. HIFU monotherapy showed the greatest median reductions in wrinkles and pores, whereas the combined protocol showed broader early changes across multiple parameters. This suggests that the sequential protocol may not necessarily outperform HIFU in every individual structural parameter but may provide a more global skin-quality response by targeting different anatomical and biological levels of skin aging.

An additional clinically relevant observation was the different immediate post-treatment skin appearance between HIFU and microneedling-assisted EXO-PDRN interventions. Immediately after HIFU treatment, minimal visible erythema or epidermal irritation was observed despite thermal stimulation of deeper dermal and subdermal tissue layers. This observation is consistent with the mechanism of focused ultrasound technology, which induces selective thermal coagulation at targeted depths while relatively preserving the epidermal surface. In contrast, microneedling-assisted EXO-PDRN produced transient diffuse erythema immediately after treatment, reflecting controlled superficial microinjury, increased microcirculation, and early wound-healing activation. These observations highlight the different anatomical targets and biological responses of the two interventions and support the rationale for investigating sequential multimodal treatment approaches.

The relatively short follow-up period is important when interpreting the findings. HIFU-induced collagen remodeling and tissue contraction are progressive biological processes that may continue for several weeks or months after treatment. Therefore, the stronger wrinkle- and pore-related reductions observed in the HIFU monotherapy group may primarily reflect early structural tightening effects. In contrast, the combined HIFU + MN–EXO-PDRN protocol may require longer follow-up to fully demonstrate its regenerative and remodeling potential. The broader early improvement profile observed in the combined protocol may therefore reflect early skin-quality recovery and regenerative response rather than maximal structural remodeling at this early evaluation timepoint.

The biological rationale for the sequential protocol is based on the complementary mechanisms of the two interventions. HIFU acts primarily through focused thermal stimulation of deeper dermal and subdermal tissues, inducing collagen fiber contraction, wound-healing activation, and progressive dermal remodeling. Microneedling, in contrast, induces controlled superficial microinjury and creates transient microchannels that may enhance the delivery and bioavailability of topical EXO-PDRN components. Exosome-based bioactive components may support intercellular regenerative signaling, while PDRN-related mechanisms may contribute to tissue repair, fibroblast activity, angiogenic signaling, and inflammatory modulation [8–15]. Therefore, the sequential use of HIFU followed by MN–EXO-PDRN may theoretically combine deeper tissue remodeling with superficial regenerative stimulation and enhanced topical delivery.

The HIFU monotherapy group showed marked changes in wrinkle-related parameters, pores, UV spots, and global pixel-based skin burden. These findings are consistent with the established mechanism of HIFU as an energy-based modality capable of inducing thermal coagulation points, collagen contraction, and subsequent neocollagenesis. The reduction in pores may reflect dermal tightening and improved perifollicular structural support, while improvement in wrinkle-related parameters likely reflects early collagen remodeling and tissue contraction. However, these findings should be interpreted within the early follow-up period of the study.

The MN–EXO-PDRN monotherapy group demonstrated moderate changes across several parameters, including sensitivity, spots, wrinkles, pores, and global pixel-based skin burden. These findings suggest that superficial microneedling at 0.5 mm, combined with EXO-PDRN application, may support early improvement in skin quality and barrier-related parameters. However, the magnitude of change was generally lower than that observed in HIFU-related structural parameters, which may be expected given the more superficial depth of intervention and the single-session design.

Another important aspect of the present study is that the MN–EXO-PDRN protocol was evaluated after a single application. Most regenerative aesthetic protocols involving microneedling, resurfacing, or bioactive exosome-based formulations commonly include repeated sessions or combination procedures [15]. Therefore, assessing the early response following a single microneedling-assisted EXO-PDRN session provides clinically relevant information regarding the short-term regenerative potential and feasibility of this approach. The findings suggest that measurable changes in several objective digital skin parameters may be observed even before completion of a repeated multi-session regenerative protocol.

Correlation analysis further supported the relationship between local parameter changes and global digital skin changes. The strongest correlation was observed between wrinkle-related changes and changes in global pixel-based skin burden, indicating that wrinkle-related improvement was closely associated with broader digital skin-quality changes. Significant correlations were also observed between pore-related changes and global pixel-based burden changes, as well as between sensitivity-related changes and global pixel-based burden changes. These findings suggest that the observed effects were not isolated to a single parameter but reflected broader changes in objective digital skin aging indices.

The use of AI-assisted digital skin analysis represents strength of the study. Traditional aesthetic assessment often relies on clinical photography and subjective evaluation, which may be influenced by lighting, positioning, evaluator bias, and patient perception. In contrast, digital skin analysis provides quantitative assessment of multiple parameters, including wrinkles, pores, spots, UV spots, porphyrins, sensitivity, and global pixel-based skin burden. Nevertheless, AI-assisted image-based assessment is not free from variability. Measurement outputs may be influenced by hydration status, environmental conditions, facial positioning, lighting consistency, and algorithm-related factors. Therefore, digital skin analysis should be interpreted as an objective supportive tool rather than as a standalone substitute for clinical evaluation.

Changes in spots and UV spots should be interpreted with caution, as these parameters represent pigmentary indices rather than primary structural remodeling outcomes. In the present study, pigmentary changes were exploratory secondary findings and should not be interpreted as evidence of a dedicated pigment-targeting effect. Established pigment-directed energy-based treatments, such as Q-switched Nd:YAG laser protocols, have been specifically developed and evaluated for hyperpigmentation and dyschromia. Cannarozzo et al. reported the use of Q-switched 1064/532 nm Nd:YAG laser as a dedicated approach for benign hypermelanosis in Asian patients [21]. Therefore, the changes observed in spots and

UV spots in the present study should be considered incidental and preliminary, requiring confirmation in future studies specifically designed to evaluate pigmentary outcomes.

Regarding the observed changes in UV spot-related parameters after HIFU, several possible explanations may be considered. First, HIFU-induced dermal remodeling may indirectly influence image-based pigmentary indices through changes in tissue architecture, skin texture, optical light reflection, and tissue repair processes. Second, previous experimental evidence has suggested that high-intensity focused ultrasound may influence UVB-induced hyperpigmentation and melanin-related skin changes, possibly through localized thermal and mechanical effects on pigment-containing structures [22]. However, in the present study, UV spot-related changes should be interpreted as exploratory imaging findings rather than as evidence that HIFU is a dedicated pigment-targeting treatment. Further studies specifically designed to evaluate pigmentation and dyschromia outcomes are required before definitive conclusions can be drawn.

The apparent increases observed in selected control-group parameters, including sensitivity and wrinkle-related values, should also be interpreted cautiously. Given the short follow-up period, these changes should not be considered definitive evidence of biological skin deterioration. Instead, they may reflect measurement variability, short-term intra-individual skin fluctuations, and differences in hydration status, environmental exposure, facial positioning, lighting-related variability, and limitations inherent to AI-assisted image-based skin analysis. Therefore, the control group findings should be viewed as an exploratory reference rather than as evidence of clinically meaningful worsening over 40 days.

Limitations

Several limitations of the present study should be acknowledged. First, this was a pilot study with a relatively small sample size, limiting the statistical power and generalizability of the findings. Second, treatment allocation was not randomized; therefore, selection bias cannot be excluded. Third, the follow-up period was limited to early outcomes, whereas HIFU-induced collagen remodeling may continue for several months after treatment. Fourth, only a single treatment session was evaluated, while regenerative aesthetic protocols frequently involve repeated sessions in clinical practice.

In addition, although AI-assisted digital skin analysis provides objective quantitative assessment, device-based measurements may still be influenced by biological and technical variables, including environmental conditions, facial positioning, lighting consistency, skin hydration, and algorithm-related factors. Therefore, short-term changes observed in untreated participants should be interpreted cautiously and require confirmation in larger studies with repeated measurements. In one participant, wrinkle-related values showed transient worsening at early follow-up, which may reflect timing-related variability during the early remodeling phase.

No standardized skincare or sunscreen regimen was provided, and participants maintained their usual skincare routines. This may have introduced minor variability in skin hydration, barrier status, and photoprotection during follow-up. Finally, the absence of histological or molecular biomarker evaluation limits interpretation of the underlying biological mechanisms associated with the observed clinical improvements.

5. Conclusions

Within the limitations of this pilot comparative clinical study, all active intervention protocols demonstrated measurable improvement in objective digital skin aging parameters compared with controls. HIFU monotherapy showed the strongest reduction in wrinkle- and pore-related parameters, while the sequential HIFU + MN–EXO-PDRN proto-

col demonstrated broader early improvement across multiple indices, including sensitivity, wrinkles, pores, UV spots, and global pixel-based skin burden.

These findings suggest that combining deeper energy-based dermal remodeling with superficial regenerative stimulation and enhanced topical delivery may provide a more global skin quality response than single-modality approaches alone. Correlation analysis further supported the relationship between local parameter improvement and overall reduction in digital skin burden, particularly between wrinkle reduction and global pixel-based skin burden improvement.

In addition, the use of AI-assisted digital skin analysis enabled objective quantitative assessment of treatment-related changes and highlights the growing role of digital technologies in regenerative aesthetic research. Although preliminary, the present findings support the potential clinical value of sequential multimodal regenerative protocols combining HIFU with microneedling-assisted EXO-PDRN. Future randomized controlled studies with larger populations, repeated treatment sessions, longer follow-up, and molecular or histological evaluation are warranted to further clarify the clinical efficacy and biological mechanisms underlying these interventions.

Author Contributions: Conceptualization, F.B. and E.P.; methodology, F.B.; software, E.G.P.; validation, F.B., A.V. and E.P.; formal analysis, F.B. and E.G.P.; investigation, F.B.; resources, F.B.; data curation, F.B. and A.V.; writing—original draft preparation, F.B.; writing—review and editing, A.V.; visualization, A.C.L.; supervision, A.C.L.; project administration, F.B. and A.C.L. All authors have read and agreed to the published version of the manuscript.

Funding: This research received no external financial funding. The microneedling device, regenerative topical formulations, and digital skin analysis system were provided as in-kind support by Medidrops Group Greece.

Institutional Review Board Statement: The study was conducted in accordance with the Declaration of Helsinki and approved by the Bioethics and Ethics Committee of the Medical School of the National and Kapodistrian University of Athens, Greece (Approval No. 1249/29.06.2026).

Informed Consent Statement: Written informed consent was obtained from all participants involved in the study. Written informed consent was also obtained for the publication of anonymized clinical photographs and digital skin analysis images.

Data Availability Statement: The data presented in this study are available from the corresponding author upon reasonable request, subject to ethical and privacy restrictions.

Acknowledgments: The authors would like to thank Medidrops Group Greece for providing in-kind support through the devices and materials used in this study.

Conflicts of Interest: F.B. collaborates with Medidrops. Medidrops provided the Micropen EVO Revance device, EXO-PDRN formulation, topical concentrate, and MEICET Pro-D skin analyzer as in-kind support for the study. Medidrops had no role in the study design, data collection, and statistical analysis, interpretation of results, manuscript preparation, or decision to submit the article for publication.

Abbreviations

The following abbreviations are used in this manuscript:

EXO	Exosome-based components
PDRN	Polydeoxyribonucleotide
MN	Microneedling
HIFU	High-Intensity Focused Ultrasound
MN–EXO-PDRN	Microneedling-assisted exosome/polydeoxyribonucleotide therapy
HIFU + MN–EXO-PDRN	Sequential HIFU followed by microneedling-assisted EXO-PDRN therapy

UV	Ultraviolet
SD	Standard deviation
IQR	Interquartile range
AI	Artificial intelligence
MEICET Pro-D	Digital skin analysis system used for objective skin imaging and assessment
Nd:YAG	Neodymium-doped yttrium aluminum garnet

References

1. Shin, J.W.; Kwon, S.H.; Choi, J.Y.; Na, J.I.; Huh, C.H.; Choi, H.R.; Park, K.C. Molecular Mechanisms of Dermal Aging and Antiaging Approaches. *Int. J. Mol. Sci.* **2019**, *20*, 2126. [CrossRef] [PubMed]
2. Shin, S.H.; Lee, Y.H.; Rho, N.K.; Park, K.Y. Skin Aging from Mechanisms to Interventions: Focusing on Dermal Aging. *Front. Physiol.* **2023**, *14*, 1195272. [CrossRef] [PubMed]
3. Biskanaki, F.; Chaniotis, D.; Anastasiou, I.A.; Tentolouris, N.; Papadopoulos, V.; Skouras, G.; Mavreli, A.M.; Chaniotis, F.; Protopapa, E.; Lazaris, A.C. HIFU and the Oxidative Echo: A Pilot Investigation of Free Radical Stress in Facial and Neck Procedures. *Appl. Sci.* **2026**, *16*, 1558. [CrossRef]
4. Byun, J.W.; Kang, J.; Park, S.; Hong, W. Efficacy of Radiofrequency Combined with Single-Dot Ultrasound for Skin Rejuvenation: A Non-Randomized Split-Face Trial with Blinded Response Evaluation. *Ski. Res. Technol.* **2023**, *29*, e13461.
5. Yi, K.H.; Kim, E.; Wan, J.; Lee, A.W.K.; Yang, Y.C.; Lu, S.P.H.; Huang, J.; Huang, P.H.P.; Peng, H.L.P. Noninvasive High-Intensity Focused Ultrasound for Skin Brightening Efficacy Using a Topical Agent Containing Glutathione and Hyaluronic Acid. *J. Dermatol. Treat.* **2024**, *35*, 2406932. [CrossRef] [PubMed]
6. Aldawood, F.K.; Andar, A.; Desai, S. A Comprehensive Review of Microneedles: Types, Materials, Processes, Characterizations and Applications. *Polymers* **2021**, *13*, 2815. [CrossRef] [PubMed]
7. Lim, D.J.; Kim, H.J. Microneedles in Action: Microneedling and Microneedles-Assisted Transdermal Delivery. *Polymers* **2022**, *14*, 1608. [CrossRef] [PubMed]
8. Kalluri, R.; LeBleu, V.S. The Biology, Function, and Biomedical Applications of Exosomes. *Science* **2020**, *367*, eaau6977. [CrossRef] [PubMed]
9. Zhang, B.; Shi, Y.; Gong, A.; Pan, Z.; Shi, H.; Yang, H.; Fu, H.; Yan, Y. Exosomes-Based Advancements for Application in Medical Aesthetics. *Front. Bioeng. Biotechnol.* **2022**, *10*, 1083640. [CrossRef] [PubMed]
10. Pinto, H.; Sánchez-Vizcaíno Mengual, E. Exosomes in the Real World of Medical Aesthetics: A Review. *Aesthetic Plast. Surg.* **2024**, *48*, 2513–2527. [CrossRef] [PubMed]
11. Hu, S.; Li, Z.; Cores, J.; Huang, K.; Su, T.; Dinh, P.U.; Cheng, K. Needle-Free Injection of Exosomes Derived from Human Dermal Fibroblast Spheroids Ameliorates Skin Photoaging. *ACS Nano* **2019**, *13*, 11273–11282. [CrossRef] [PubMed]
12. Kwon, H.H.; Yang, S.H.; Lee, J.; Park, B.C.; Park, K.Y.; Jung, J.Y.; Bae, Y.; Park, G.H. Combination Treatment with Human Adipose Tissue Stem Cell-Derived Exosomes and Fractional CO_2 Laser for Acne Scars: A 12-Week Prospective, Double-Blind, Randomized, Split-Face Study. *Acta Derm. Venereol.* **2020**, *100*, adv00310. [CrossRef] [PubMed]
13. Park, S.; Baek, S.; Shin, H.-J.; Kim, J.-S.; Gwon, H.-I.; Bae, S.; An, S. Polydeoxyribonucleotides as Emerging Therapeutics for Skin Diseases: Clinical Applications, Pharmacological Effects, Molecular Mechanisms, and Potential Modes of Action. *Appl. Sci.* **2025**, *15*, 10437. [CrossRef]
14. Veronesi, F.; Dallari, D.; Sabbioni, G.; Carubbi, C.; Martini, L.; Fini, M. Polydeoxyribonucleotides from Skin to Musculoskeletal Tissue Regeneration via Adenosine A2A Receptor Involvement. *J. Cell. Physiol.* **2017**, *232*, 2299–2307. [CrossRef] [PubMed]
15. Kimbrell, M.L. Enhanced Healing and Outcomes with Human Dermal Fibroblast Exosomes: Case Series Combining Deep Helium Radiofrequency Plasma Skin Resurfacing, Facelifts, and Exosomes. *Aesthet. Surg. J.* **2026**, *46*, S73–S81. [CrossRef] [PubMed]
16. Henseler, H. Validation of the Visia® Camera System for Skin Analysis through Assessment of the Different Skin Signs. *Ski. Res. Technol.* **2022**, *28*, 835–842.
17. Zawodny, P.; Stój, E.; Kulig, P.; Skonieczna-Żydecka, K.; Sieńko, J. VISIA Skin Analysis System as a Tool to Evaluate the Reduction of Pigmented and Vascular Skin Lesions after Laser Therapy. *Clin. Cosmet. Investig. Dermatol.* **2022**, *15*, 1479–1491.
18. Henseler, H. Measurement of the Effects of a Skin Care Regimen Using the Visia® Camera System. *Int. Plast. Reconstr. Surg.* **2022**, *11*, e170.
19. Eldridge, S.M.; Chan, C.L.; Campbell, M.J.; Bond, C.M.; Hopewell, S.; Thabane, L.; Lancaster, G.A. CONSORT 2010 Statement: Extension to Randomised Pilot and Feasibility Trials. *BMJ* **2016**, *355*, i5239. [CrossRef] [PubMed]
20. Teresi, J.A.; Yu, X.; Stewart, A.L.; Hays, R.D. Guidelines for Designing and Evaluating Feasibility Pilot Studies. *Med. Care* **2022**, *60*, 95–103. [CrossRef] [PubMed]

21. Cannarozzo, G.; Del Re, C.; Negosanti, F.; Bennardo, S.; Amoruso, G.F.; Nisticò, S.P.; Bennardo, L. Q-Switched Nd:YAG laser to Manage Hyperpigmentation in Asians: A Multicenter Study. *Cosmetics* **2023**, *10*, 44. [CrossRef]
22. Choi, S.Y.; Kim, K.H.; Kim, K.H.; Kim, H.J.; Park, S.H.; Lee, J.H. High-intensity focused ultrasound as a potential new modality for the treatment of pigmentary skin disorder. *Ski. Res. Technol.* **2016**, *22*, 131–136. [CrossRef] [PubMed]